Rapid Communications

Superconducting pairing in Sr_2RuO_4 from weak to intermediate coupling

Li-Da Zhang,[1] Wen Huang,[2,*] Fan Yang,[1,†] and Hong Yao[2,3,‡]
[1] *School of Physics, Beijing Institute of Technology, Beijing 100081, China*
[2] *Institute for Advanced Study, Tsinghua University, Beijing 100084, China*
[3] *State Key Laboratory of Low Dimensional Quantum Physics, Tsinghua University, Beijing 100084, China*

(Received 14 October 2017; published 27 February 2018)

The unconventional superconductivity in Sr_2RuO_4 continues to attract considerable interest. Although many measurements can be interpreted on the basis of chiral p-wave pairing with intriguing topological character, a number of exceptions hinder an unambiguous verification of such pairing. The pairing mechanism also remains under debate. In this Rapid Communication, with effects of the sizable spin-orbit coupling accounted for, we reexamine the superconducting instabilities in Sr_2RuO_4 through systematic microscopic analysis within the random-phase approximation. Our calculations show that the odd-parity p-wave pairing is favored in the regime of extremely weak interactions, but that highly anisotropic even-parity pairings become most leading over a broad range of stronger interactions. These results could shed light on the nature of the enigmatic superconductivity in Sr_2RuO_4.

DOI: 10.1103/PhysRevB.97.060510

The superconductivity in Sr_2RuO_4 has attracted significant attention since it was discovered in 1994 [1–3]. The discovery was followed by proposals of p-wave pairing arising from possible remnant ferromagnetic correlations in the material [4–6], which was later substantiated by experimental evidences of spin-triplet and odd-parity pairings [7–11]. The observation of time-reversal symmetry breaking [12,13] raised the prospect of topological chiral p-wave pairing which supports Majorana fermions [14,15]. However, despite much progress, the chiral p-wave order has not been fully established, largely due to the difficulties in reconciling it with a variety of other measurements [16–19]. We highlight some major issues below.

A major prediction for the chiral p wave is the appearance of spontaneous chiral currents at the edges and domain walls separating regions of opposite chiralities [20,21]. However, no clear signature of a chiral current has been detected so far [22–24]. We stress that, as the current is not topologically protected [25], it can be suppressed, to various degrees, by gap and band-structure anisotropies, surface disorder, and the multiband effects [25–31]. However, acquiring full consistency with the experimental null result in the best prepared sample/device is perhaps only possible with a fine-tuned gap structure. Remarkably, the edge current could vanish in non-p-wave chiral superconductors, such as chiral d and f waves, etc. [32–35]. Yet these states may be less likely in Sr_2RuO_4 [32].

Another discrepancy is the absence of split transitions when an in-plane magnetic field or a uniaxial strain breaks the degeneracy between the two chiral components [36–42]. A further puzzle is the anomalous suppression of the in-plane upper critical field H_{c2} [43] at low temperatures and a related first-order nature of the superconducting transition [38,44,45]. The suppression of the in-plane H_{c2} was also implicated in the vortex lattice anisotropy throughout the mixed state [46,47]. These resemble the Pauli limiting behavior and can usually be tied to spin-singlet pairing but may also be explained if the $\boldsymbol{d}$ vector of the spin-triplet pairing lies on the plane—which however corresponds to a time-reversal invariant helical state. Equally intriguing is the evidence of line nodes [48–50], whereas the chiral p wave is typically fully gapped except in special cases where anisotropy introduces accidental nodes or deep gap minima [51].

Part of the complication arises from the multiband nature [52], which hinders unambiguous interpretations of some of the experiments. Since early times it was pointed out [53] that superconductivity is most likely dominated by one set of the three metallic bands, given the disparity of the quasi-one-dimensional (quasi-1D) and quasi-two-dimensional bands. By interband scattering, pairing can also develop on the subdominant band(s) with a weaker amplitude [54]. However, there seems to be no consensus regarding the identification of the primary superconducting band(s). The van Hove singularity on the γ band and the wall of enhanced spin fluctuations between $\boldsymbol{Q}_1 \approx (2/3,2/3)\pi$ and $\boldsymbol{Q}_2 \approx (\pi,2k_F)$ associated with the quasi-1D bands [55–57] were argued to promote independent pairing instabilities, including the p wave, on the respective band(s). There are different recent theoretical works in support of both scenarios [58–61].

Recent weak-coupling renormalization-group (RG) calculations [62,63] found the leading p-wave state to develop similar gap amplitudes on all three bands. In these calculations, the limit $U/W \ll 1$ where W is the bandwidth (or $U/t \ll 1$ where t is the primary hopping amplitude) [64] is taken. Under the assumption that the bare on-site Coulomb interactions do not affect (see later) the superconducting solutions resultant from particle-hole density-wave fluctuations, for $U/t \to 0$ it suffices to perform a calculation up to the one-loop level, and the solution is considered asymptotically exact in the absence of competing particle-hole instabilities.

*huangw001@mail.tsinghua.edu.cn
†yangfan_blg@bit.edu.cn
‡yaohong@tsinghua.edu.cn

However, in reality Coulomb interactions in Sr_2RuO_4 may not be that weak. In particular, the bare interactions in multi-band or multiorbital systems may contribute either repulsive or attractive effective interactions in certain pairing channels, which may affect the predictions based on density-wave-fluctuation mechanisms. Additionally, higher-order scatterings associated with the finite interactions are expected to introduce corrections to the structure of the interactions. This may be particularly important in the present multiband system wherein multiple pairing instabilities likely coexist. To this end, we perform systematic calculations using the random-phase approximation (RPA) to analyze the leading pairing symmetries as a function of interaction strength from weak to nearly intermediate interactions. The important microscopic details, such as the spin-orbit coupling (SOC), are fully accounted for. Our most important finding is an emerging trend: a crossover from p-wave pairing at extremely weak U to highly anisotropic even-parity s- and d-wave pairings at relatively stronger and likely more physically relevant U. Our results therefore hold important implications for the pairing theories of Sr_2RuO_4.

Model. The band structure of Sr_2RuO_4 is described by the following three-orbital tight-binding Hamiltonian on a square lattice:

$$H = \sum_{\boldsymbol{k},s} \psi^{\dagger}_{\boldsymbol{k},s} \hat{H}_{0s}(\boldsymbol{k}) \psi_{\boldsymbol{k},s}, \tag{1}$$

where the spinor $\psi_{\boldsymbol{k},s} = (c_{xz\boldsymbol{k},s}, c_{yz\boldsymbol{k},s}, c_{xy\boldsymbol{k},-s})^T$ with $c_{a\boldsymbol{k},s}$ annihilating a spin-s electron on the a orbital ($a = xz,yz,xy$), $s = \uparrow$ and $\downarrow$ denote up and down spins, and,

$$\hat{H}_{0s}(\boldsymbol{k}) = \begin{pmatrix} \xi_{xz,\boldsymbol{k}} & \lambda_{\boldsymbol{k}} - is\eta & i\eta \\ \lambda_{\boldsymbol{k}} + is\eta & \xi_{yz,\boldsymbol{k}} & -s\eta \\ -i\eta & -s\eta & \xi_{xy,\boldsymbol{k}} \end{pmatrix}, \tag{2}$$

with $\xi_{xz,\boldsymbol{k}} = -2t \cos k_x - 2\tilde{t} \cos k_y - \mu$, $\xi_{yz,\boldsymbol{k}} = -2\tilde{t} \cos k_x - 2t \cos k_y - \mu$, $\lambda_{\boldsymbol{k}} = -4t'' \sin k_x \sin k_y$, $\xi_{xy,\boldsymbol{k}} = -2t'(\cos k_x + \cos k_y) - 4t''' \cos k_x \cos k_y - \mu_1$. Here $\lambda_{\boldsymbol{k}}$ is the interorbital hybridization between the two quasi-1D xz and yz orbitals, and η is the strength of SOC which is found to be sizable [65–67]. Note that because SOC mixes different spins on the xy and the other two orbitals, the spins are not good quantum numbers. However, since the Kramers degeneracy on each band is preserved, it is convenient to adopt a pseudospin notation where the electrons on the Bloch bands are denoted pseudo-spin-up and pseudo-spin-down fermions. We fix the band parameters: $(t,\tilde{t},t',t''',\mu,\mu_1) = (1,0.1,0.8,0.3,1,1.1)t$ which are known to capture the overall band structure and Fermi-surface geometry of Sr_2RuO_4 [68–70]. For now we leave undetermined the magnitude of the orbital mixing t'' and η. Their values will be suitably tuned to analyze the influence of the associated microscopic details.

We consider the on-site Coulomb interactions between the Ru t_{2g} orbitals as the following:

$$\begin{aligned} H_{\text{int}} = &\sum_{i,a,s\neq s'} \frac{U}{2} n_{ias} n_{ias'} + \sum_{i,a\neq b,s,s'} \frac{U'}{2} n_{ias} n_{ibs'} \\ &+ \sum_{i,a\neq b,s,s'} \frac{J}{2} c^{\dagger}_{ias} c^{\dagger}_{ibs'} c_{ias'} c_{ibs} \\ &+ \sum_{i,a\neq b,\, s\neq s'} \frac{J'}{2} c^{\dagger}_{ias} c^{\dagger}_{ias'} c_{ibs'} c_{ibs}, \end{aligned} \tag{3}$$

where i is the site index, $a,b = xz,yz,xy$, $n_{ias} \equiv c^{\dagger}_{ias} c_{ias}$. Throughout this Rapid Communication we assume $U' = U - 2J$ and $J' = J$ where J is the Hund's coupling.

To study the superconducting instabilities, we obtain effective pairing vertices using systematic RPA calculations formulated in the pseudospin language (see the Supplemental Material [71]), which differ from the previous RPA and perturbative expansion studies [72–74]. Note that, as the atomic SOC does not break inversion symmetry, notions of odd- and even-parity pairings remain valid and are in one to one correspondence with *pseudo-spin-triplet* and *pseudo-spin-singlet* pairings. Accordingly, the obtained gap functions acquire the standard forms $\hat{\Delta}^t_{\boldsymbol{k}} \sim i(\boldsymbol{\sigma} \cdot \boldsymbol{d}_{\boldsymbol{k}})\sigma_y$ and $\hat{\Delta}^s_{\boldsymbol{k}} \sim i\,\Delta_{\boldsymbol{k}}\sigma_y$, which are expressed in the pseudospin basis. The forms of $\boldsymbol{d}_{\boldsymbol{k}}$ and $\Delta_{\boldsymbol{k}}$ fall in the irreducible representations of the D_{4h} crystalline symmetry group, and the orientation of the $\boldsymbol{d}$ vector ($\boldsymbol{d}_{\boldsymbol{k}}$) represents the pseudospin configuration of the odd-parity pairing. The simple chiral p wave is given by $(k_x \pm ik_y)\hat{z}$, whereas the helical p-wave states are marked by in-plane $\boldsymbol{d}$ orientations: $k_x\hat{x} \pm k_y\hat{y}$ and $k_y\hat{x} \pm k_x\hat{y}$.

To deduce the general behavior, we perform calculations using orbital mixing parameters in the range of $t'',\eta \in (0,0.15)t$. Figure 1 depicts the phase diagrams in terms of the dimensionless interaction parameters J/U and $\lg(U/t)$ for four sets of (t'',η), which are roughly representative of our overall observation. In the following we separately discuss the two limiting cases: extreme weak U [i.e., $\lg(U/t) < -1$ or $U < 0.1t$] and finite U [i.e., $\lg(U/t) > -1$].

Weak-U limit. In the extreme weak-coupling limit, the p-wave gap functions obtained in our calculations are in excellent agreement with the previous study [62] [see Fig. 2(b)]. In the presence of sizable SOC, the three bands are more prompt to develop comparable gaps. The SOC also induces anisotropic spin correlations [75–77] responsible for the splitting between the chiral and the helical channels. Naturally, the balance between the two is sensitive to SOC, which acts in conjunction with other microscopic details in the band structure and the bare interactions, such as t'' and J/U. Crudely speaking, the chiral p-wave state wins over the helical p-wave state at smaller J/U's, and stronger SOC tips the balance towards a helical p wave [Figs. 1(a)–1(c)]. The former is consistent with the previous study which found leading chiral and helical pairings for small and larger J/U's, respectively. In addition, at larger t'''s, the chiral state develops more favorably than the helical pairing, and more p-wave phase space becomes overtaken by even-parity pairing [see Figs. 1(b) and 1(d)]. The sensitivity to the microscopics was also noted in a recent work [78].

As a crucial remark, at the RPA level treated here the spin fluctuations *on their own* in fact favor even-parity s- or d-wave pairing, instead of p-wave pairing. In these extreme weak-U calculations, the p-wave pairing surpasses the others because the even-parity channels are suppressed by nonvanishing repulsive components at the bare-U level. We have verified this via explicit calculations where only the bare-U contribution is included and where it is purposely taken out. Hence caution is needed when interpreting the extreme weak-U results.

Intermediate U. Most important of all, a robust emerging trend, irrespective of the details of the orbital mixing, is the crossover at relatively weak interaction strength from p-wave to s- and d-wave pairings which are in the A_{1g} and B_{1g}

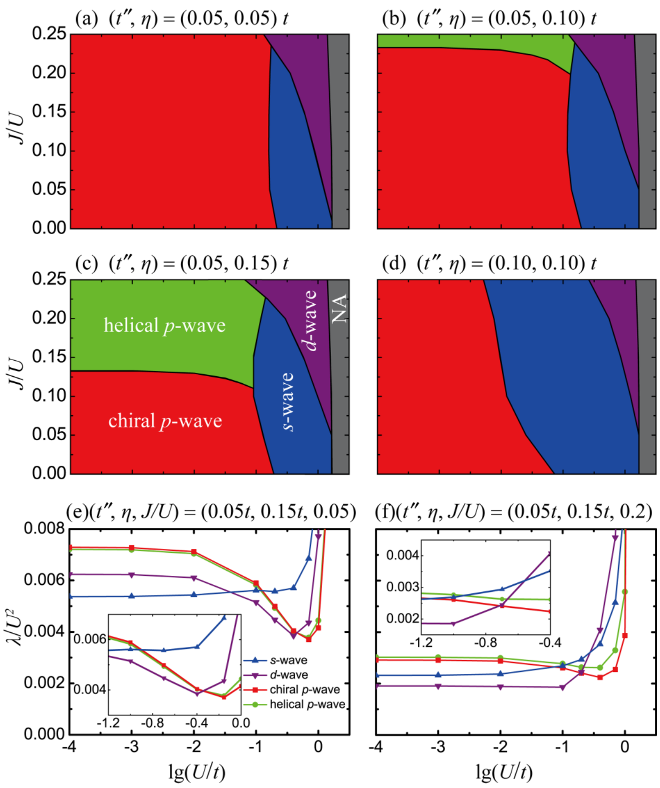

FIG. 1. Phase diagrams as a function of the interaction parameters J/U and $\lg(U/t)$ for (a) $(t'',\eta) = (0.05,0.05)t$, (b) $(0.05,0.10)t$, (c) $(0.05,0.15)t$, and (d) $(0.10,0.10)t$. Only the single most leading channel at each point is indicated [see the text in (c) for labels]: chiral p wave (red), helical p wave (green), s wave (blue), $d_{x^2-y^2}$ wave (purple), and "NA" (gray) correspond to the regime where the RPA susceptibility diverges and where our method breaks down. The phase boundaries are rough estimates. They are smoothed lines connecting the approximate midpoints which separate our data points (see the Supplemental Material [71]) associated with different phases. (e) and (f) evolution of the eigenvalues of the gap equation in different channels as a function of the interaction parameter $\lg(U/t)$. Note the logarithmic scale on the x axis.

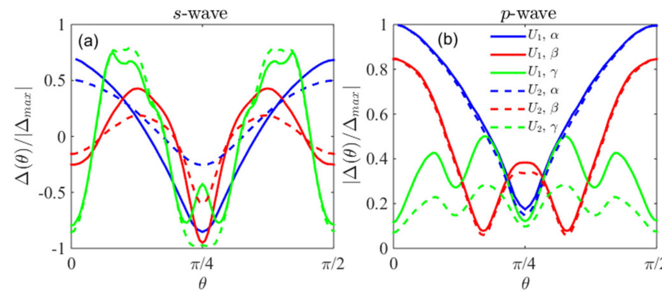

FIG. 2. The s- and p-wave gaps as a function of the angle with respect to the k_y axis at two different interaction parameters $U = U_1 = 0.01t$ (the solid curves) and $U = U_2 = 0.2t$ (the dashed curves). The calculations are performed with $(t'',\eta) = (0.05,0.15)t$ and $J/U = 0.1$. Note that the s wave is the third and first leading states at U_1 and U_2, respectively; whereas the p wave is the first and second states.

representations, respectively. In addition, the d-wave pairing is increasingly favored at larger J/U's (Fig. 1), and the s-wave channel invariably exhibits strong gap anisotropy with multiple accidental nodes across the Fermi surfaces [e.g., Figs. 2(a) and 3(b)]. These constitute the central message of the present Rapid Communication. Some of the representative gap functions are depicted in Figs. 3(a)–3(c).

Typically on the order of $U = U_0 \sim 0.1t$ [Figs. 1(e) and 1(f)], the spin-fluctuation-mediated effective interactions begin to supersede the bare-U repulsion in several even-parity channels. Note that, although at this order the bare-U interactions are still relatively strong compared with $O(U^2)$, their components in the respective eigenchannels can be much weaker. Across U_0, the obtained gap structure exhibits quantitative variations in, e.g., the detailed shape and the relative amplitudes of the gaps across the three bands as is illustrated in Fig. 2.

Since the bare-U interactions have no effect on the p-wave pairing, variations in this channel must result exclusively from the higher-order corrections in RPA. The inaction of bare U permits a stronger statement that the p-wave pairing must be driven by spin fluctuations alone. Traces of this mechanism [30,61] can be found in, e.g., the approximate relation $\mathrm{sgn}[\Delta_{\boldsymbol{k}}] = \mathrm{sgn}[\Delta_{\boldsymbol{k}+\boldsymbol{Q}}]$ in the near-nested portions of the quasi-1D Fermi surfaces as indicated by the arrows in Fig. 3(a). A similar degree of RPA correction is expected for even-parity pairings. However, since the bare-U repulsion and the spin-fluctuation-mediated interactions "interfere" nontrivially in these channels, it was not until at somewhat larger U's where the latter dominates. For example, as shown in Fig. 3(c) for a model with $U = t$ which develops sizable pairing gaps on the quasi-1D bands, the nested regions satisfy $\mathrm{sgn}[\Delta_{\boldsymbol{k}}] = -\mathrm{sgn}[\Delta_{\boldsymbol{k}+\boldsymbol{Q}}]$ characteristic of an even-parity pairing favored by the momentum-$\boldsymbol{Q}$ spin fluctuations.

However, care must be taken when attributing the superconductivity to certain spin-fluctuation modes as the interactions in this multiorbital system are inherently multiband in nature (except in the strong-U limit where a single mode prevails) [63]. The multiband effects may operate differently in different channels, which is best illustrated by comparing the γ-band pairing in single- and multiband models. Its van Hove singularity induces spin fluctuations not only at small momenta, but also at large wave vectors surrounding (π,π) [41]. Depending on the interaction strength and the exact filling fraction, these fluctuations may support s-, p-, or d-wave channels within the RPA [71]. The gap functions are plotted along with the multiband results in Figs. 3(d)–3(f). Obviously, distinctions appear not only around the locus of maximal band mixing, but also away from them, despite very similar γ-band spin fluctuations in the two models [71]. Especially, the contrast is much more appreciable in the p- and d-wave channels, suggesting stronger multiband effects at play in the two.

It will be stressed that the multiband character persists, irrespective of the distribution of the gaps on the three bands which, by contrast, is not generic. Depending on the parametrization of the orbital mixing, the pairing can reside primarily on one set of bands or be of similar magnitude on all three. On the one hand, stronger SOC in general leads to more comparable gap amplitudes; on the other hand, since the momentum-dependent xz/yz-orbital hybridization $\lambda_{\boldsymbol{k}}$ destroys the α/β-band nesting conditions more dramatically with larger t'''s as the pairings on these two bands are increasingly suppressed compared to that on γ.

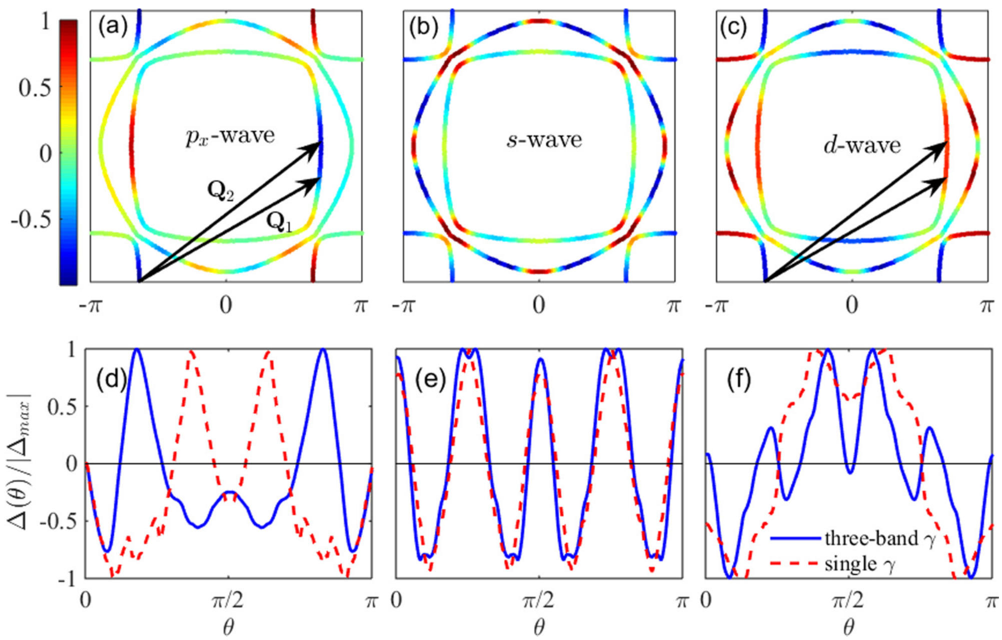

FIG. 3. Upper panel: leading RPA gap functions in three regions of interaction strength: (a) $U = 10^{-4}t$, (b) $U = 0.1t$, and (c) $U = t$ wherein the three-band model gives most leading chiral p-wave (shown is the p_x-component), s-, and $d_{x^2-y^2}$-wave pairings, respectively. Lower panel: comparison of γ-band gap functions obtained in the three-band model (the solid curves) and an effective one-band model (the dashed curves), under the same interaction strength in correspondence with those in the upper panels. In the plots shown, the three-band model assumes interband mixing $(t'',\eta) = (0.05,0.15)t$, and the interaction parameter J/U is held fixed at 0.1. The one-band model uses a band structure and a filling fraction that resemble those of the γ band. Its leading channel is always the d wave at the chosen filling level, $\mu_1 = 1.1t$ (see the Supplemental Material [71]) with subdominant p- and s-wave pairings. The wave-vectors $\boldsymbol{Q}_1$ and $\boldsymbol{Q}_2$ shown in (a) and (c) are approximately equal to those mentioned in the text up to a reciprocal lattice wave vector.

Other symmetries. Planar chiral f-wave pairings in product representations, taking the forms of $(k_x^2 - k_y^2)(k_x + ik_y)\hat{z}$ and $k_xk_y(k_x + ik_y)\hat{z}$ [79,80], were proposed to explain the reported low-temperature thermodynamic and transport measurements [48–50]. However, we did not find these pairings among the most leading channels obtained in our calculations.

Implications for RG studies. In the $U/t \to 0$ limit within the regime of validity of the two-stage weak-coupling RG developed in Ref. [58], one first integrates out the states with energies higher than an artificial cutoff $\Omega_0 \ll U^2/t$. This generates a low-energy effective action from which one computes the RG flow of the individual Cooper channels. Since $\Omega_0 \to 0$, we expect the existing weak-coupling RG study as formulated in Ref. [62] to yield the same results as our RPA as it did. In the intermediate range of U still far from particle-hole instabilities, e.g., $0.1 < U/t < O(1)$ in the present Rapid Communication [81], the system can still be viewed as weakly coupled. However, the perturbative treatment of the high-energy modes must now be carried out more accurately. For example, Zanchi and Schulz [82] implemented a standard one-loop RG calculation for the high-energy states down to a physical cutoff, below which the flow of the particle-hole loops disappear exponentially. Given the nontrivial interplay of the bare-U and higher-order interactions found in the RPA, a corresponding study within the RG is naturally of considerable interest and will be pursued separately.

The functional RG approaches [60,61] by contrast use sizable U. In addition, they take into account the interplay between the pairing and the particle-hole channels in the RG flow—an ingredient missing in the weak-coupling RG. In these studies, the growth of the odd-parity pairing channel is found to be faster than that of the even-parity ones as the temperature or cutoff energy decreases. However, although both yield leading p waves, they disagree on which set of bands drives the pairing. Inferring from our results, this could potentially originate from the different microscopic details adopted in the two studies. It therefore seems important to attend to the microscopics and scan over a broader parameter range in order to obtain a complete phase diagram.

Concluding remarks. The leading pairing obtained in our RPA appears in the p-wave channel in the extreme weak-coupling regime and in even-parity s- or d-wave channels in a broad range of intermediate interactions—in contrast with the widely held assumption for Sr_2RuO_4. We do note that multiple signatures inconsistent with the chiral p wave may go very well with even-parity pairing. For example, taken at face value, these pseudo-spin-singlet states are in line with the suppression of the in-plane H_{c2} and the character of first-order superconducting transition at low temperatures [38,43–45,83,84], although these behaviors may also be explained by invoking an orbital polarization mechanism due to finite SOC [85]. Moreover, the obtained gap functions in these channels exhibit multiple accidental (s-wave) or symmetry-imposed (d-wave) vertical line nodes, which may explain the residual density of states [48–50]. In addition, on a tetragonal lattice as in Sr_2RuO_4, planar even-parity pairing belongs to the 1D irreducible representation and typically does not break time-reversal invariance; hence the superconductor is not expected to generate the chiral current at the edges nor split transitions in the presence of C_4 symmetry-breaking perturbations.

Although it is still premature to draw a firm conclusion of alternative pairing symmetry in this material due to the obvious reason that even-parity pairing cannot be straightforwardly reconciled with the many observations in support of p-wave pairing, our results call for new perspectives in studying the superconductivity in Sr_2RuO_4. As a side remark, our Rapid Communication also shows how the pairing in a multiband superconductor can be strongly influenced by the multiband interactions.

Acknowledgments. We would like to acknowledge helpful communications with J. Berlinsky, I. Eremin, C. Kallin, K. Machida, T. Scaffidi, M. Sigrist, S. Simon, Y. Tanaka, and F.-C. Zhang. This Rapid Communication was supported by NSFC under Grant No. 11604013 (L.-D.Z.) and Grants No. 11674025, No. 11334012, and No. 11274041 (F.Y.), Beijing Natural Science Foundation under Grant No. 1174019 (L.-D.Z.), and the C. N. Yang Junior Fellowship at Tsinghua University (W.H.).

[1] Y. Maeno, H. Hashimoto, K. Yoshida, S. Nishizaki *et al.*, Nature (London) **372**, 532 (1994).
[2] Y. Maeno, T. M. Rice, and M. Sigrist, Phys. Today **54**(1), 42 (2001).
[3] A. P. Mackenzie and Y. Maeno, Rev. Mod. Phys. **75**, 657 (2003).
[4] T. M. Rice and M. Sigrist, J. Phys.: Condens. Matter **7**, L643 (1995).
[5] G. Baskaran, Physica B (Amsterdam) **223-224**, 490 (1996).
[6] M. Cuoco, C. Noce, and A. Romano, Phys. Rev. B **57**, 11989 (1998).
[7] K. Ishida, H. Mukuda, Y. Kitaoka, K. Asayama, Z. Q. Mao, Y. Mori, and Y. Maeno, Nature (London) **396**, 658 (1998).
[8] J. A. Duffy, S. M. Hayden, Y. Maeno, Z. Mao, J. Kulda, and G. J. McIntyre, Phys. Rev. Lett. **85**, 5412 (2000).
[9] K. D. Nelson, Z. Q. Mao, Y. Maeno, and Y. Liu, Science **306**, 1151 (2004).
[10] K. Ishida, M. Manago, T. Yamanaka, H. Fukazawa, Z. Q. Mao, Y. Maeno, and K. Miyake, Phys. Rev. B **92**, 100502(R) (2015).
[11] M. Manago, K. Ishida, Z. Q. Mao, and Y. Maeno, Phys. Rev. B **94**, 180507(R) (2016).
[12] G. M. Luke, Y. Fudamoto, K. M. Kojima *et al.*, Nature (London) **394**, 558 (1998).
[13] J. Xia, Y. Maeno, P. T. Beyersdorf, M. M. Fejer, and A. Kapitulnik, Phys. Rev. Lett. **97**, 167002 (2006).
[14] N. B. Kopnin and M. M. Salomaa, Phys. Rev. B **44**, 9667 (1991).
[15] N. Read and D. Green, Phys. Rev. B **61**, 10267 (2000).
[16] C. Kallin and A. J. Berlinsky, J. Phys.: Condens. Matter **21**, 164210 (2009).
[17] Y. Maeno, S. Kittaka, T. Nomura, S. Yonezawa, and K. Ishida, J. Phys. Soc. Jpn. **81**, 011009 (2012).
[18] C. Kallin, Rep. Prog. Phys. **75**, 042501 (2012).
[19] A. P. Mackenzie, T. Scaffidi, C. W. Hicks, and Y. Maeno, npj Quantum Materials **2**, 40 (2017).
[20] M. Matsumoto and M. Sigrist, J. Phys. Soc. Jpn. **68**, 994 (1999).
[21] A. Furusaki, M. Matsumoto, and M. Sigrist, Phys. Rev. B **64**, 054514 (2001).
[22] J. R. Kirtley, C. Kallin, C. W. Hicks, E.-A. Kim, Y. Liu, K. A. Moler, Y. Maeno, and K. D. Nelson, Phys. Rev. B **76**, 014526 (2007).
[23] C. W. Hicks, J. R. Kirtley, T. M. Lippman, N. C. Koshnick, M. E. Huber, Y. Maeno, W. M. Yuhasz, M. B. Maple, and K. A. Moler, Phys. Rev. B **81**, 214501 (2010).
[24] P. J. Curran, S. J. Bending, W. M. Desoky, A. S. Gibbs, S. L. Lee, and A. P. Mackenzie, Phys. Rev. B **89**, 144504 (2014).
[25] W. Huang, S. Lederer, E. Taylor, and C. Kallin, Phys. Rev. B **91**, 094507 (2015).
[26] P. E. C. Ashby and C. Kallin, Phys. Rev. B **79**, 224509 (2009).
[27] Y. Imai, K. Wakabayashi, and M. Sigrist, Phys. Rev. B **85**, 174532 (2012).
[28] A. Bouhon and M. Sigrist, Phys. Rev. B **90**, 220511(R) (2014).
[29] S. Lederer, W. Huang, E. Taylor, S. Raghu, and C. Kallin, Phys. Rev. B **90**, 134521 (2014).
[30] T. Scaffidi and S. H. Simon, Phys. Rev. Lett. **115**, 087003 (2015).
[31] S. B. Etter, A. Bouhon, and M. Sigrist, Phys. Rev. B **97**, 064510 (2018).
[32] W. Huang, E. Taylor, and C. Kallin, Phys. Rev. B **90**, 224519 (2014).
[33] Y. Tada, W. Nie, and M. Oshikawa, Phys. Rev. Lett. **114**, 195301 (2015).
[34] T. Ojanen, Phys. Rev. B **93**, 174505 (2016).
[35] S. I. Suzuki and Y. Asano, Phys. Rev. B **94**, 155302 (2016).
[36] M. Sigrist and K. Ueda, Rev. Mod. Phys. **63**, 239 (1991).
[37] Y. A. Ying, N. E. Staley, Y. Xin, K. Sun, X. Cai, D. Fobes, T. Liu, Z. Q. Mao, and Y. Liu, Nat. Commun. **4**, 2596 (2013).
[38] S. Yonezawa, T. Kajikawa, and Y. Maeno, J. Phys. Soc. Jpn. **83**, 083706 (2014).
[39] C. W. Hicks, D. O. Brodsky, E. A. Yelland *et al.*, Science **344**, 283 (2014).
[40] A. Steppke, L. Zhao, M. E. Barber, T. Scaffidi *et al.*, Science **355**, eaaf9398 (2017).
[41] Y. C. Liu, F. C. Zhang, T. M. Rice, and Q. H. Wang, npj Quantum Mater. **2**, 12 (2017).
[42] Y.-T. Hsu, W. Cho, A. F. Rebola, B. Burganov, C. Adamo, K. M. Shen, D. G. Schlom, C. J. Fennie, and E.-A. Kim, Phys. Rev. B **94**, 045118 (2016).
[43] K. Deguchi, M. A. Tanatar, Z. Q. Mao, T. Ishiguro, and Y. Maeno, J. Phys. Jpn. Soc. **71**, 2839 (2002).
[44] S. Yonezawa, T. Kajikawa, and Y. Maeno, Phys. Rev. Lett. **110**, 077003 (2013).
[45] S. Kittaka, A. Kasahara, T. Sakakibara, D. Shibata, S. Yonezawa, Y. Maeno, K. Tenya, and K. Machida, Phys. Rev. B **90**, 220502(R) (2014).
[46] C. Rastovski, C. D. Dewhurst, W. J. Gannon, D. C. Peets, H. Takatsu, Y. Maeno, M. Ichioka, K. Machida, and M. R. Eskildsen, Phys. Rev. Lett. **111**, 087003 (2013).
[47] S. J. Kuhn, W. Morgenlander, E. R. Louden *et al.*, Phys. Rev. B **96**, 174507 (2017).
[48] K. Ishida, Y. Kitaoka, K. Asayama, S. Ikeda, S. Nishizaki, Y. Maeno, K. Yoshida, and T. Fujita, Phys. Rev. B **56**, R505(R) (1997).
[49] S. NishiZaki, Y. Maeno, and Z. Q. Mao, J. Phys. Soc. Jpn. **69**, 572 (2000).

[50] E. Hassinger, P. Bourgeois-Hope, H. Taniguchi, S. René de Cotret, G. Grissonnanche, M. S. Anwar, Y. Maeno, N. Doiron-Leyraud, and L. Taillefer, Phys. Rev. X **7**, 011032 (2017).
[51] I. A. Firmo, S. Lederer, C. Lupien, A. P. Mackenzie, J. C. Davis, and S. A. Kivelson, Phys. Rev. B **88**, 134521 (2013).
[52] K. Deguchi, Z. Q. Mao, H. Yaguchi, and Y. Maeno, Phys. Rev. Lett. **92**, 047002 (2004).
[53] D. F. Agterberg, T. M. Rice, and M. Sigrist, Phys. Rev. Lett. **78**, 3374 (1997).
[54] M. E. Zhitomirsky and T. M. Rice, Phys. Rev. Lett. **87**, 057001 (2001).
[55] T. Imai, A. W. Hunt, K. R. Thurber, and F. C. Chou, Phys. Rev. Lett. **81**, 3006 (1998).
[56] M. Braden, Y. Sidis, P. Bourges, P. Pfeuty, J. Kulda, Z. Mao, and Y. Maeno, Phys. Rev. B **66**, 064522 (2002).
[57] I. I. Mazin and D. J. Singh, Phys. Rev. Lett. **82**, 4324 (1999).
[58] S. Raghu, A. Kapitulnik, and S. A. Kivelson, Phys. Rev. Lett. **105**, 136401 (2010).
[59] J. W. Huo, T. M. Rice, and F. C. Zhang, Phys. Rev. Lett. **110**, 167003 (2013).
[60] Q. H. Wang, C. Platt, Y. Yang, C. Honerkamp, F. C. Zhang, W. Hanke, T. M. Rice, and R. Thomale, Europhys. Lett. **104**, 17013 (2013).
[61] M. Tsuchiizu, Y. Yamakawa, S. Onari, Y. Ohno, and H. Kontani, Phys. Rev. B **91**, 155103 (2015).
[62] T. Scaffidi, J. C. Romers, and S. H. Simon, Phys. Rev. B **89**, 220510(R) (2014).
[63] W. Huang, T. Scaffidi, M. Sigrist, and C. Kallin, Phys. Rev. B **94**, 064508 (2016).
[64] S. Raghu, S. A. Kivelson, and D. J. Scalapino, Phys. Rev. B **81**, 224505 (2010).
[65] M. W. Haverkort, I. S. Elfimov, L. H. Tjeng, G. A. Sawatzky, and A. Damascelli, Phys. Rev. Lett. **101**, 026406 (2008).
[66] C. N. Veenstra *et al.*, Phys. Rev. Lett. **112**, 127002 (2014).
[67] C. G. Fatuzzo *et al.*, Phys. Rev. B **91**, 155104 (2015).
[68] A. Damascelli *et al.*, Phys. Rev. Lett. **85**, 5194 (2000).
[69] C. Bergemann *et al.*, Adv. Phys. **52**, 639 (2003).
[70] C. Bergemann, S. R. Julian, A. P. Mackenzie, S. NishiZaki, and Y. Maeno, Phys. Rev. Lett. **84**, 2662 (2000).
[71] See Supplemental Material at http://link.aps.org/supplemental/10.1103/PhysRevB.97.060510 for more details, which includes Refs. [86–95].
[72] T. Takimoto, Phys. Rev. B **62**, R14641(R) (2000).
[73] T. Nomura and K. Yamada, J. Phys. Soc. Jpn. **69**, 3678 (2000).
[74] T. Nomura and K. Yamada, J. Phys. Soc. Jpn. **71**, 1993 (2002).
[75] K. K. Ng and M. Sigrist, Europhys. Lett. **49**, 473 (2000).
[76] I. Eremin, D. Manske, and K. H. Bennemann, Phys. Rev. B **65**, 220502(R) (2002).
[77] S. Cobo, F. Ahn, I. Eremin, and A. Akbari, Phys. Rev. B **94**, 224507 (2016).
[78] Y.-T. Hsu, A. F. Rebola, C. J. Fennie, and E.-A. Kim, arXiv:1701.07884.
[79] Y. Hasegawa, K. Machida, and M. Ozaki, J. Phys. Soc. Jpn. **69**, 336 (2000).
[80] M. J. Graf and A. V. Balatsky, Phys. Rev. B **62**, 9697 (2000).
[81] Note that in our RPA calculations the peak value of the bare susceptibility components (S9) typically does not exceed ~ 0.5 for $0.1 < U/t < O(1)$.
[82] D. Zanchi and H. J. Schulz, Phys. Rev. B **54**, 9509 (1996).
[83] Y. Amano, M. Ishihara, M. Ichioka, N. Nakai, and K. Machida, Phys. Rev. B **91**, 144513 (2015).
[84] N. Nakai and K. Machida, Phys. Rev. B **92**, 054505 (2015).
[85] A. Ramires and M. Sigrist, Phys. Rev. B **94**, 104501 (2016).
[86] T. Takimoto, T. Hotta, and K. Ueda, Phys. Rev. B **69**, 104504 (2004).
[87] K. Yada and H. Kontani, J. Phys. Soc. Jpn. **74**, 2161 (2005).
[88] K. Kubo, Phys. Rev. B **75**, 224509 (2007).
[89] K. Kuroki, S. Onari, R. Arita, H. Usui, Y. Tanaka, H. Kontani, and H. Aoki, Phys. Rev. Lett. **101**, 087004 (2008).
[90] S. Graser, T. A. Maier, P. J. Hirschfeld, and D. J. Scalapino, New J. Phys. **11**, 025016 (2009).
[91] T. A. Maier, S. Graser, P. J. Hirschfeld, and D. J. Scalapino, Phys. Rev. B **83**, 100515(R) (2011).
[92] F. Liu, C.-C. Liu, K. Wu, F. Yang, and Y. Yao, Phys. Rev. Lett. **111**, 066804 (2013).
[93] X. Wu, J. Yuan, Y. Liang, H. Fan, and J. Hu, Europhys. Lett. **108**, 27006 (2014).
[94] T. Ma, F. Yang, H. Yao, and H. Lin, Phys. Rev. B **90**, 245114 (2014).
[95] L.-D. Zhang, F. Yang, and Y. Yao, Sci. Rep. **5**, 8203 (2015).